5 CASE STUDY 1: Characterisation of parameters influencing the performance of the Owlstone FAIMS sensor

5.1 Introduction

As introduced in Chapter 1, and explored throughout Chapter 2, the geometry of a field asymmetric ion mobility spectrometry (FAIMS) sensor affects its performance. The Owlstone FAIMS sensor possesses the smallest geometry of any such device currently available and so it is both interesting and scientifically valuable to investigate the consequences of the development.

Through the theoretical equations detailed in Chapter 2 it is possible to draw general trends of behaviour. Experimental investigations, however, allow the assessment of varying specific parameters without requiring an exhaustive knowledge of all the variables within a system.

To understand the inter-related dependencies concerning the modification of the carrier flow in analysis including the Owlstone FAIMS sensor a systematic investigation was undertaken. The specific parameters investigated were the pressure, humidity and magnitude of the air flow used as the carrier flow. It was known through the expressions in Chapter 2 that these parameters would affect the residence time, clustering and E/N environment within the FAIMS sensor. With this study it was anticipated that the interplay between the parameters would be exposed and the effect upon the product ion response's compensation voltage (CV), full width at half maximum (FWHM) and intensity would be revealed.

For the work in this chapter a single analyte was selected for study. The compound chosen was dimethylmethylphosphonate (DMMP, Table 5.1) because of its association with the traditional applications of FAIMS, homeland defence. This means that there is a wealth of published material within the literature which could be used to aid in the understanding of the data obtained. Additionally, results obtained would potentially be relevant to future investigations within the largest application of FAIMS technology.

5.1.1   General properties of DMMP

The motivation for studying DMMP in previous ion mobility work has been that it is thermally stable, has low reactivity with water and that it is a simulant for the nerve agent sarin [1]. DMMP is easier to handle within the laboratory than sarin and considerably less dangerous, but, still behaves in a similar way within a FAIMS instrument. Table 5.1 details some of the general properties of DMMP as well as the structure of sarin for comparison.

Table 5.1 General properties of DMMP

Properties	
Molecular formula	$C_3H_9O_3P$
Molar mass	124.08 g/mol
Density	1.16 g/ml
Boiling point	181°C
Structure: DMMP	
Structure: sarin	
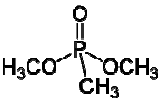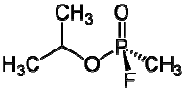
At room temperature DMMP is liquid, which meant that a trace analyte vapour could be reliably provided through a permeation source.

5.1.2   The response of DMMP in a FAIMS system

Figure 5.1 displays the DF sweep of DMMP from three separate studies. Figure 5.1 a) and

b) are taken from the literature and Figure 5.1 c) was obtained from an Owlstone Lonestar

unit, as part of the investigation detailed later in this chapter.
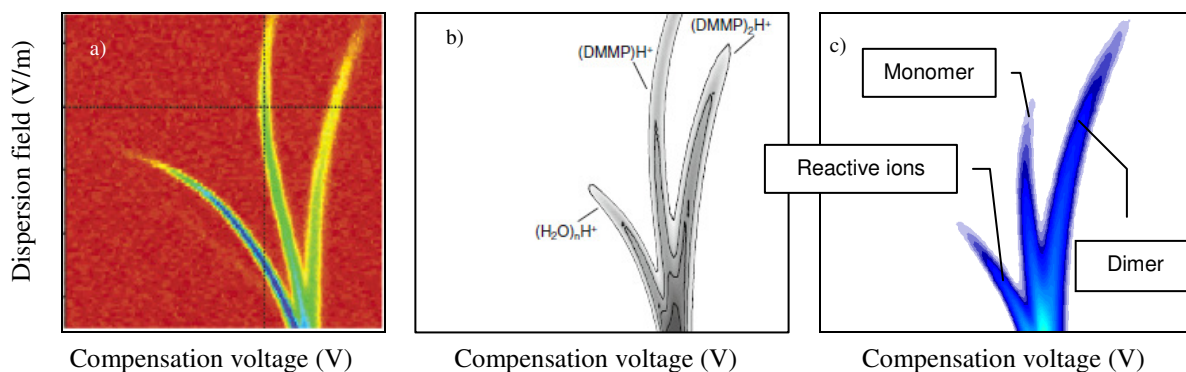
Figure 5.1 DMMP response in positive polarity under various conditions with a carrier flow of air. a) taken from Nazarov *et al.* using the Sionex SVAC FAIMS unit [2] b) taken from An *et al.* [3], again using a Sionex SVAC unit c) obtained through an Owlstone Lonestar unit.

Despite the variation in the colour maps used to describe ion intensity in the different

investigations all are from the positive mode. DMMP only produces positive product ions

so only the positive polarity will be considered throughout this chapter.

The conditions employed in each investigation are all different so direct comparison is

difficult. However, the general forms of all three dispersion field (DF) sweeps are

remarkably similar. All consist of three prominent ion species. These three ion species are

considered to be the reactive ion reservoir and the monomer and dimer product ions (as

labelled in Figure 5.1 c)). The chemical identity of each species is described by the labels

within Figure 5.1 b), which can include various additional levels of hydration [2-5]. The

evolution of the reactive and dimer ion species is described by a continuous migration to

greater negative and positive CV values with increasing DF strength respectively. The

monomer ion species is different as it initially migrates to increasingly negative CV values

but later turns back and moves to more positive CV values with increasing DF strength.

173

The behaviour of each ion species is a result of the specific α function with the energy available to the ion through the ratio *E/N* (Section 2.5.3).

5.2   Operation

An understanding of the results obtained in this chapter requires a description of the processes used in obtaining the data and their analysis. This includes recounting the methods employed through data collection, the assessment of errors and how data were restricted to constant *E/N* environments.

A full description of the apparatus used within this study was presented within Table 3.1 and detailed within Section 3.6. Blank responses and investigations into the systems stability were provided in Sections 3.6.2 and 3.6.3 respectively.

5.2.1   Data collection

Three DF sweeps were taken for each arrangement of the apparatus, with 100 CV sweeps between 1 - 100% of the maximum DF. Obtaining full DF sweeps in this manner meant that individual CV sweeps could be easily isolated, to maintain a constant *E/N*. The motivation for this is discussed later in Section 5.2.3.

The majority of the CV spectra collected included mixed responses from separate ion species. It was therefore necessary to employ the peak fitting methods reported in Chapter 4 to obtain the most accurate and relevant data possible. Specifically, the differential peak fitting method was implemented and the peak amplitude, peak position, FWHM and peak area was recorded for each Gaussian peak fitted. Figure 5.2 gives an example of the results obtained through this peak fitting.
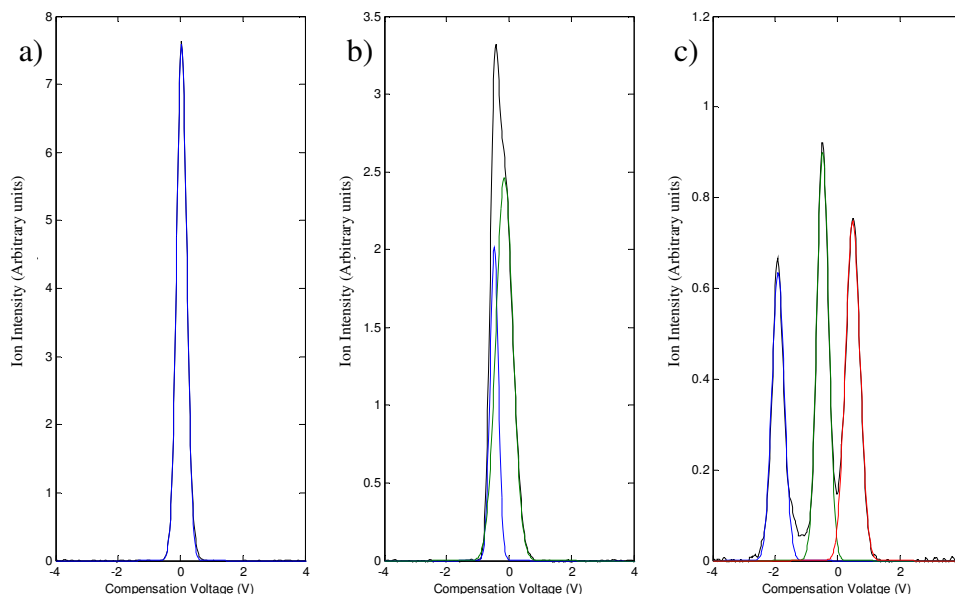
Figure 5.2 Example results of peak fitting on responses obtained from DMMP at DF strengths of a) 10 b) 30 and c) 50% of the maximum electric field strength. Original CV sweep are shown within each trace (black).

Following the peak fitting the properties of the individual Gaussian peaks were extracted.

5.2.2   Calculation of errors

Owing to the number of different parameters of the apparatus it would have been difficult and potentially less accurate to approximate an error from combining individual errors from the apparatus (*e.g.* reading error). Instead, where errors are presented within graphical plots they are a single standard deviation of the three runs undertaken at identical conditions. While this is a quantitative assessment of the repeatability of the apparatus it does not address the error involved in the setting of parameters between runs. An example of this would be how accurately the pressure of the carrier flow was returned to a particular value following a different setting. To address this, an investigation was undertaken where the parameters were reset between runs to understand the reproducibility of the procedure. In this way the pressure and magnitude of the carrier flow were investigated across a range. It was discovered that the error obtained was typically twice as great as the variation

encountered through continuous operation of the apparatus. This body of data could not be as complete as the assessment of repeatability so the error in the reproducibility is not provided within any of the plots within this chapter. There will, however, occasionally be a mention of the reproducibility within the main text.

The level of humidity within the carrier flow was accurately measured through testing the carrier with an external humidity sensor (Section 3.3.5) prior to the analyte flow being integrated for analysis. However, because the humidity was being generated through dynamic headspace the particular humidity present was dependent upon several factors including the agitation of the water reservoir and temperature of the laboratory. It was therefore possible to encourage a humidity value within a range but extremely laborious to fix an exact value. Hence, humidity was accurately recorded but not accurately selected. As a consequence, there is no assessment of the reproducibility with respect to humidity since there was no attempt to repeat a humidity setting after the humidity had been altered.

5.2.3   Equivalent *E/N*

To facilitate comparison of the data; as many variables were kept constant as possible, so that any trends could be correctly assigned to the variable under study. From FAIMS theory the ratio of electric field strength over number density of neutrals (*E/N*) affects the mobility of an ion-molecule, and is dependent upon pressure, through *N*. To investigate the effects of varying pressure a method of maintaining the *E/N* ratio had to be implemented. A solution was to observe the FAIMS response at a DF strength which maintained the *E/N* ratio to a reference condition. The selection of the reference condition will be described shortly but first the method of calculating the appropriate DF strength is presented.

The DF used by the Lonestar software is described as a percentage of the maximum possible by the unit. The DF strength is also linearly proportional to the electric field, so that if the DF is doubled the electric field imposed is also doubled. N is also linearly dependent upon pressure in the same way so that,

$$\frac{E}{N} = k_p \frac{DF\%}{P} \qquad\qquad 5.1$$

Where E is the electric field strength, P is the pressure and k_p is the constant of proportionality equal to $\frac{k_b T V_{max}}{100 \cdot g}$ (where V_{max} is the maximum possible voltage, g is the gap height and k_b is the Boltzmann constant).

Now, with a selected ratio of $DF\%/P$, if the pressure is changed the appropriate DF% can be selected to maintain the ratio, which in turn ensures E/N is maintained. Within this chapter when a constant E/N environment is discussed it will be presented in units of Townsends (Td), where $1\ Td = 1 \times 10^{-17}$ V·cm². Effort was invested to consider the E/N ratio in terms of experimental parameters to simplify the procedure through experimentation. A graphical representation of what is occurring to the velocity and displacement of ions, with respect to electric field strength and pressure, is provided in Appendix I.

Following preliminary work three reference conditions were selected for other readings to be normalised to. Each represents interesting experimental features and is confined by limitations imposed by the apparatus. For example, selecting a reference at too high a DF strength would limit how much the pressure could be increased despite the limits of the apparatus not being matched, confining the potential breadth of the study. Limiting the

number of references to three enabled snapshots of the evolution of ion responses but also

kept the data to a manageable quantity for assessment.

Specifically, the three references were selected as 10, 30 and 50% of the maximum DF, at

a pressure of 120 kPa. The equivalent Townsend values for the three references are 23.0,

66.5 and 100.2 Td respectively. Figure 5.3 shows the three reference conditions in relation

to the response from DMMP at a carrier flow pressure of 120 kPa.
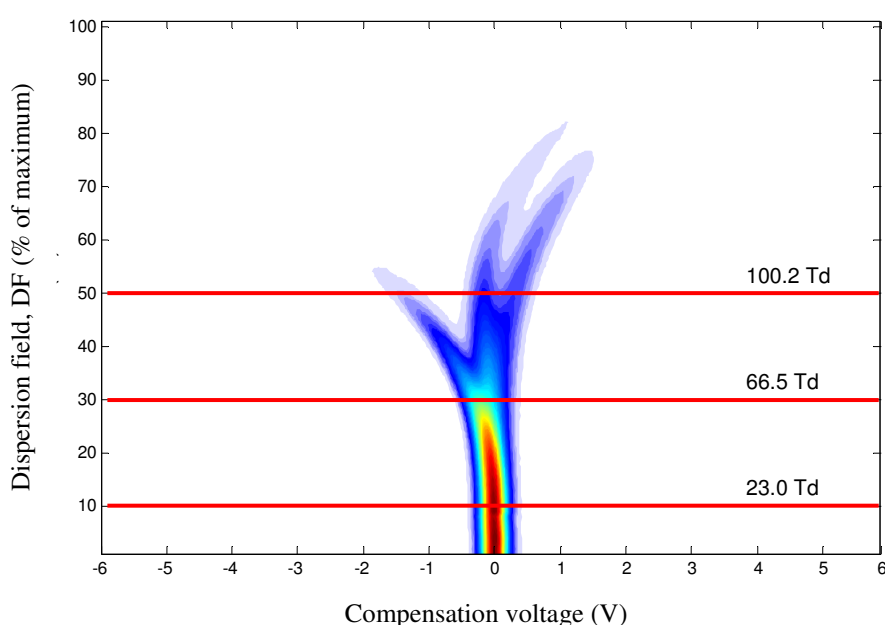
Figure 5.3 DF sweep of DMMP at a pressure of 120 kPa. The horizontal red lines depict the reference points used to assess responses under different conditions.

These reference points were chosen because they correspond to (a) a fully mixed ion

response (23.0 Td), (b) a point where it is possible to witness the beginning of resolution

between the reactant and product ions (66.5 Td) and (c) a fully resolved analyte with a

slight contribution from the reactant ions (100.2 Td). Peak fits of the CV spectra obtained

at the reference points were presented in Figure 5.2. Additionally, the maximum pressure

that could be accommodated in the apparatus was 240 kPa, which corresponds to a

required DF% value of 100% when using the 100.2 Td reference.

A potential drawback to concentrating on just three reference conditions is that any complicated behaviour may be difficult to discover because the environments studied are across such a span that short period behaviour cannot be observed. While this was initially thought to be a cause for concern, the typical gradual change in ion behaviour during a DF sweep meant that such variation in behaviour was not anticipated. Sudden changes in ion identity, such as those found with methyl salicylate, were not expected in the E/N ranges investigated [2]. Additionally, the reported loss of the DMMP dimer following its breakdown at high temperatures was not anticipated because analysis was carried out at a sensor temperature and E/N environments too small for it to become prominent [3].

5.3   Preliminary investigations

Before a full study was conducted, preliminary investigations were undertaken to test the procedure and apparatus described previously. These investigations looked at varying the pressure and magnitude of carrier flow upon the formation of the reactant ions.

5.3.1   Ion intensity of reactant ion peak

Figure 5.4 shows the peak of the reactant ion peak (RIP) response across a range of pressures and magnitudes of the carrier flow provided to the Lonestar unit. The data presented is from an E/N of 66.5 Td, data from all three references displayed the same behaviour.
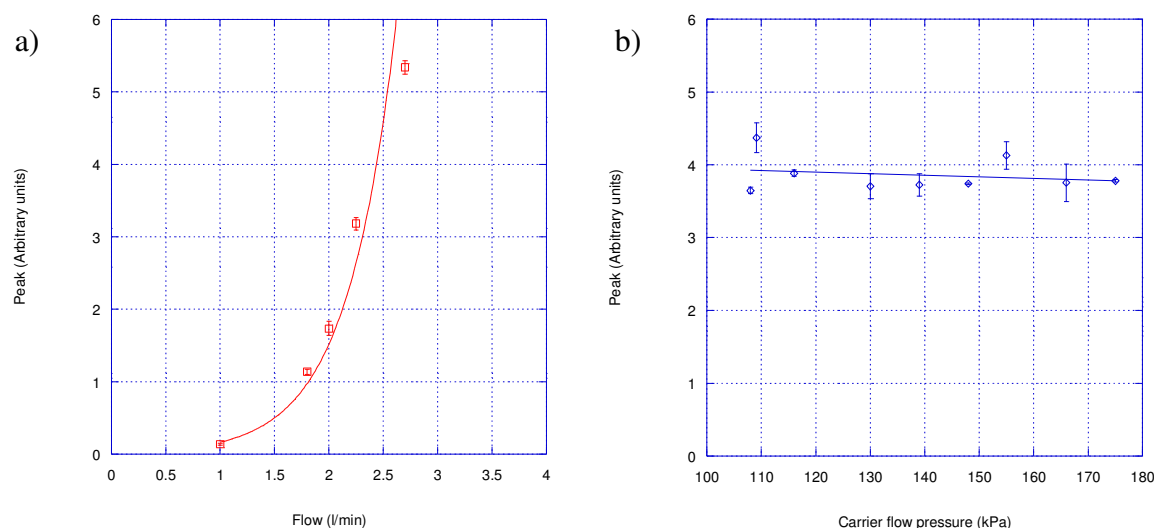
Figure 5.4 All readings taken at 66.5 Td. a) Peak of RIP response where flow was held constant at 2.5 l/min (blue diamonds with linear line of best fit) and b) peak of RIP response, where pressure was held constant at 120 kPa (red squares with exponential line of best fit).

The lines of best fit, exponential (variable flow) and linear (variable pressure), are included as an aid to trace the response.

The ion intensity of the reactive ions with respect to the pressure and magnitude of the carrier flow revealed dependence on both parameters. An increase in the flow rate resulted in a strong increase in the ion intensity of the reactant ions. This was primarily attributed to a reduction in the residence time of ions within the FAIMS sensor. As flow through the sensor increases the residence time of the ions decrease meaning there is less opportunity for diffusion. Diffusion leads to a loss of ions suitable for transmission, as random interactions with the neutral carrier gas can cause neutralisation at a sensor wall (Section 2.9). It is not expected that signal intensity will continue to increase in such a dramatic way, with forever increasing quantities of carrier flow, but over the range investigated a strong increase is maintained. It is expected that the ion intensity will reach a maximum with increasing flow rate as turbulence will eventually develop causing increased losses of reactive ions, as predicted through application of the Reynolds number (Section 2.6.2).

This observed behaviour of ion intensity with respect to magnitude of flow, residence time and diffusion losses has been described previously in the literature [6].

From Figure 5.4 a) it was also clear that poor sensitivity resulted from low flow rates. A good reservoir of reactive ions would be essential for the formation of product ions in later investigations and so the minimum flow used from this point on was 1.5 l/min. This meant that responses of variable flow all occurred in the approximately linear region of response (1.5 - 2.5 l/min). Flows below 1 l/min fall below the suggested operational parameters of the Lonestar but were investigated here for completeness.

Increasing the pressure of carrier flow led to a consistent but small decrease in ion intensity. The effect was, however, less prominent than changing the magnitude of carrier flow. The variation in pressure was carried out at a constant magnitude of flow so the residence time of ions would have been identical across the range. Nevertheless, loss of sensitivity was again attributed to diffusion within the separation region. With an increase in pressure the ions would be more likely to interact with the neutrals present. The greater number of interactions would result in a larger likelihood that an ion could experience a change in trajectory that leads to a collision with a sensor wall.

5.3.2   CV position of reactant ions

Ion species with different mobilities are characterised by the CV required to permit their passage through the FAIMS sensor. CV is therefore an important quantity to determine and it is valuable to understand how it can be affected by the variation of specific parameters.

The CV displacement (zero displacement taken as the CV value with no electric field imposed) of the data previously presented in Figure 5.4 are provided within Figure 5.5. The humidity of the carrier flow was unmodified from the laboratory compressed air supply (~10 ppm).
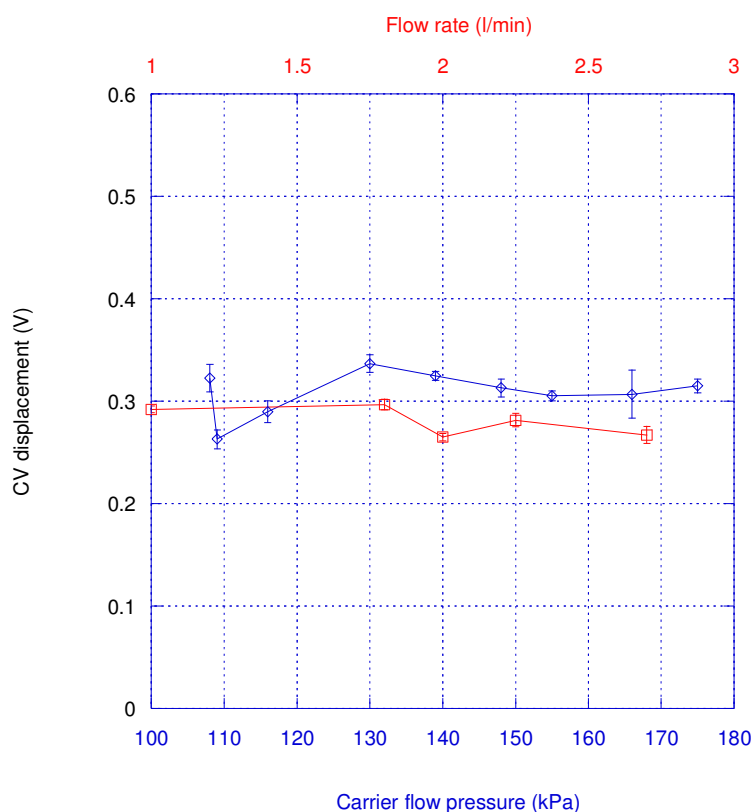
Figure 5.5 CV displacement of the same data presented within Figure 5.4, variable carrier flow pressure (blue diamonds, flow = 2.5 l/min) and variable flow (red sqaures, pressure = 120 kPa). All readings taken at 66.5 Td.

The data presented in Figure 5.5 was all recorded at a constant *E/N* ratio of 66.5 Td. This means that the energy available to the reactant ions is consistent throughout. There is no clear dependence of CV displacement with the magnitude or pressure of the carrier flow. The data obtained from the other reference conditions show a similar relationship.

The apparent independence of CV, with respect to carrier flow magnitude and pressure, suggested that there would be no improvement in resolution through modification of the carrier flow. These measurements were, however, undertaken at a low humidity and as

examples within the literature have shown, greater levels of humidity can lead to a change in the CV position of ions [5, 7-9].

The finding that there was no dependence of CV with respect to the carrier flow rate is in disagreement with the results reported by Miller *et al*. for an early micro-machined FAIMS system [6]. Within their source the CV is described as dependent upon the residence time, and hence flow rate, within the separation region. Here it is argued that while the net displacement of an ion with a trajectory unsuitable for detection is dependent upon the residence time, the CV is not. This is because, for detection, an ion must have an equal transverse displacement within the FAIMS sensor in both the high and low field regions of the applied waveform. Since the compensating field is consistently being applied to the ion, it is continuously being brought central to the separation region after each waveform, and therefore the compensation required is independent of how many waveforms the ion has undergone. This means that the CV position of an ion is independent of the flow rate. Miller *et al*. concluded that the possible variation in CV displacement could also be due to the onset of turbulence. Following this preliminary investigation, it is proposed that the observed dependence on carrier flow rate for the CV position of the ion response by Miller *et* al. was entirely the result of turbulence. As investigated and presented within Section 2.6.2 turbulent flow is not expected with any of the work undertaken within this thesis.

It is also important to note that a reduction in CV displacement was not observed across the carrier flow pressure, which is evidence that the ions experience a constant energy, suggesting the procedure employed to ensure a consistent E/N environment is successful.

The above findings merited further investigation; this involved the monitoring of CV positions after the introduction of both analyte and humidity (to investigate the potential

effect of clustering). However, these preliminary results indicated that the system was

stable and that the set-up was suitable for the later experimentation.

5.3.3   FWHM of reactant ions

To complete the understanding of the response from the FAIMS sensor, the variability of

the FWHM with respect to the carrier flow was investigated. The FWHM of the same ion

responses previously discussed in Sections 5.3.1 and 5.3.2 are given in Figure 5.6.
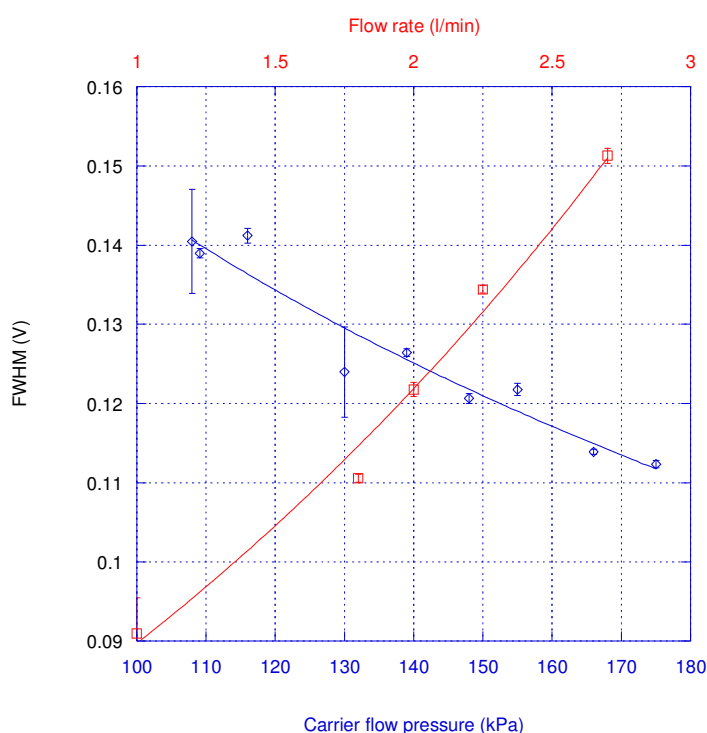
Figure 5.6 FWHM of the same data presented within Figure 5.4, variable carrier flow pressure (blue diamonds, flow = 2.5 l/min) and variable flow (red squares, pressure = 120 kPa). All readings taken at 66.5 Td.

The lines of best fit are logarithmic (variable pressure) and exponential (variable flow) and

are included as an aid to trace the response. There is a clear dependence of the FWHM

with both a change in pressure and magnitude of the carrier flow.

The observed increase in the FWHM with greater magnitudes of the carrier flow is exactly as expected. This is because as the residence time of the ions within the separation region decreases the ions within the sensor undergo less filtering waveforms; also, there is less time for ions to be lost through the effects of diffusion.

With an increase in the pressure of the carrier flow, even though the residence time is constant throughout, increased diffusion of the reactant ions will occur through the rise in the number of interactions with the neutral constituents present. An increase in these interactions will result in an increase in the loss of ions that stray most from the centre of the separation region and so a greater carrier flow pressure results in a decreased FWHM.

Similar to the signal intensity, both the effects attributable to the magnitude and pressure of the carrier flow have been linked to a change in diffusional losses. However, the extent that they are evident, relative to one another, is markedly different.

5.4   Introduction of DMMP

Following the initial investigation into the behaviour of the reactant ions with respect to variation of the flow and pressure of the carrier flow, the influence of humidity and introduction of analyte was also investigated. With the introduction of analyte (DMMP 99.9%, Sigma Aldrich) it now became possible to witness whether the trends observed with the reactant ions were representative of a full analysis. Also, investigating humidity meant that it was possible to determine if the phenomenon of clustering (Section 2.3.5) was feasible within the Owlstone sensor.

5.4.1 DF sweeps with DMMP

Before specific E/N environments were isolated, a broader appreciation of the effects of changing the carrier flow parameters was pursued. This less focused approach helped provide an overview, enabling future findings to be placed within a wider context. All this was simply accomplished by looking at the full DF sweeps and sequentially varying each of the three carrier flow parameters under study. Figure 5.7 shows three separate DF sweeps with successively increasing flow.
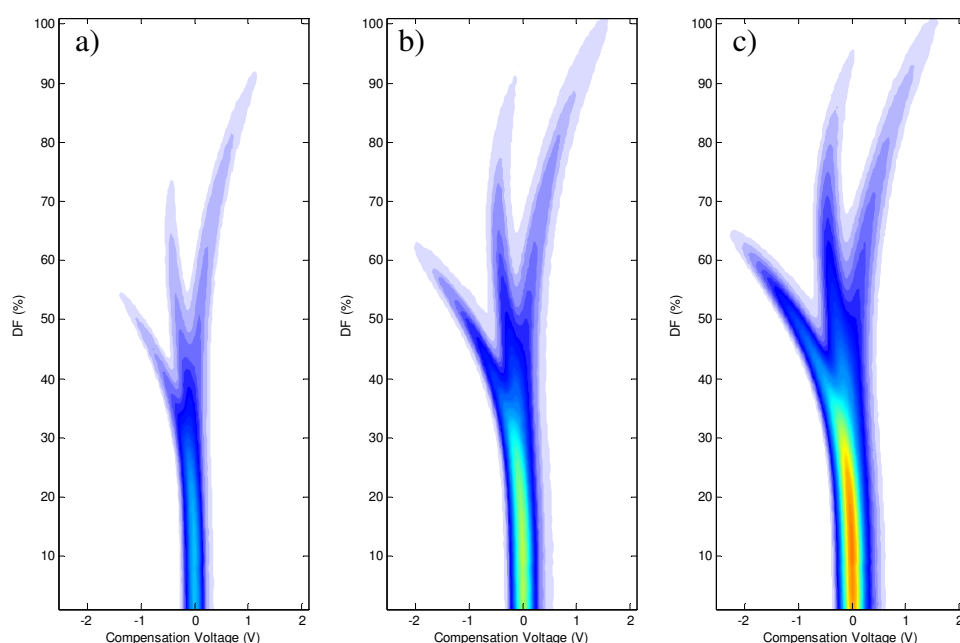
Figure 5.7 Full DF sweeps of DMMP with a carrier flow of air (at a pressure of 180 kPa) in the positive polarity. a) flow rate of 1.5 l/min and humidity of 32 ppm, b) flow rate of 2 l/min and humidity of 24 ppm and c) flow rate of 2.5 l/min and humidity of 19 ppm.

In agreement with the investigation into the reactant ions the ion intensity was observed to increase while the CV positions of the observed peaks remained unchanged. There is an increase in the FWHM of the peaks but this was again expected following the preliminary work (Section 5.3.3).

Another effect of increasing the flow appears to be an increase in the formation of the monomer relative to the dimer ion species. This may be a result of the dimer being preferentially lost through diffusion or, alternatively, it could be a result of the interactions within the ionisation region. The formation of dimer product ions requires an additional successful interaction compared to a monomer. Reducing the residence time potentially decreases the dimer population as there is less time available for the full chain of reactions to occur within the ionisation region.

Figure 5.8 shows the DF sweeps resulting from the successive increase of pressure within the FAIMS sensor.
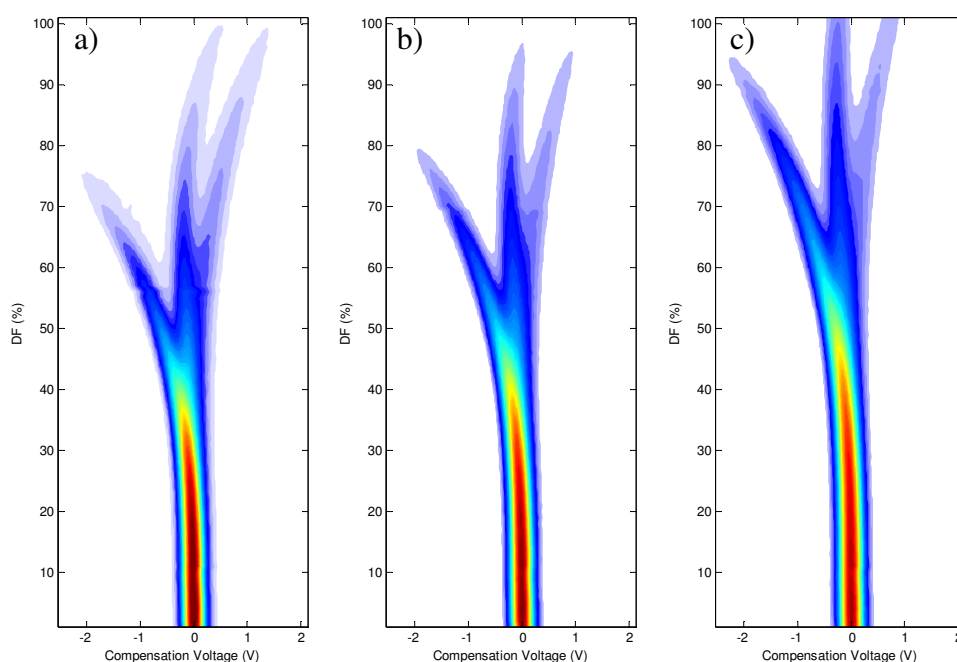
Figure 5.8 Full DF sweeps of DMMP with a carrier flow of air (at a flow of 2.5 l/min) in the positive polarity. a) carrier flow pressure of 130 kPa and humidity of 368 ppm, b) carrier flow pressure of 150 kPa and humidity of 319 ppm and c) carrier flow pressure of 180 kPa and humidity of 266 ppm.

The most immediate consequence of increasing pressure was the stretching of the spectra across the dispersion field strength. From observing where the ion species began to resolve from one another, it appears that this occurs at separate electric field strengths at different

pressures. Additionally, the ion intensity for a given DF% is greater at reduced pressures. Both these observations are a consequence of the *E/N* ratio being dependent upon pressure. For a given DF%, a) to c), the number density is increasing, resulting in less energy being imparted to the ions which results in a diminished separation. Figure 5.8 demonstrates the requirement to normalise for a particular *E/N* to enable the observation of the effects of changing the pressure of the carrier flow.

Humidity is known to play a large role within FAIMS technology [5, 9-11] and there are increasing occurrences within the literature where water has been added (as either a dopant or modifier) to control the nature of ion species created, their stability and separation [5, 8]. Figure 5.9 shows three spectra where the humidity present has been successively increased, from 19 to 1679 ppm.
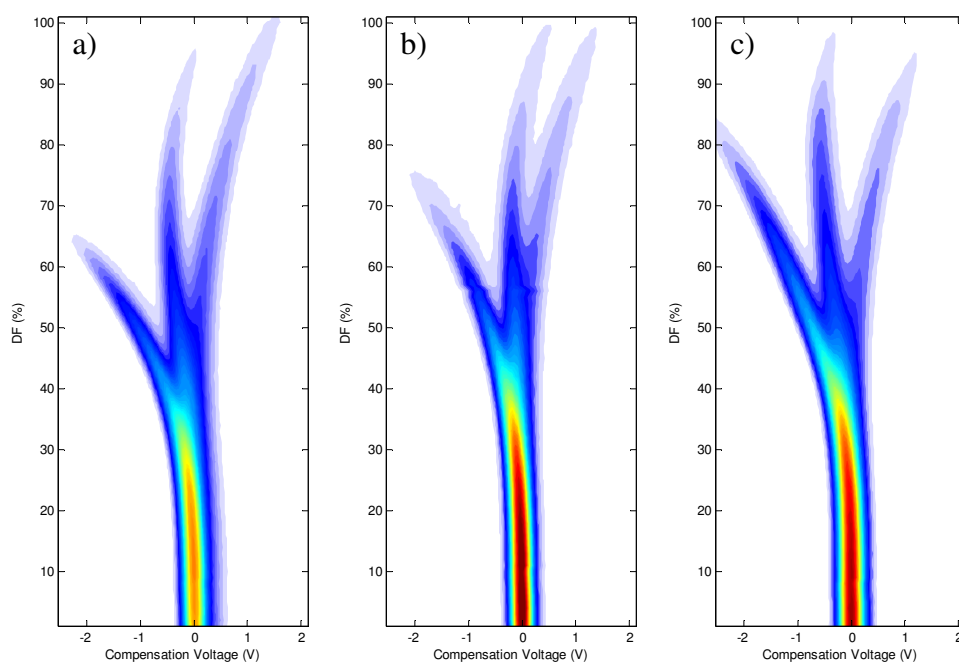
Figure 5.9 Full DF sweeps of DMMP with a carrier flow of air (at a flow of 2.5 l/min and pressure of 180 kPa) in the positive polarity. a) carrier flow humidity of 19 ppm, b) carrier flow humidity of 266 ppm and c) carrier flow humidity of 1679 ppm.

The spectra in Figure 5.9 suggest that a large change in humidity has an effect similar to that of changing the pressure. Points where the ion species begin to resolve from one another appear to occur at different DF strengths for different levels of humidity. Such a change is an indication that the net energy imparted to the ions has changed between the separate DF sweeps. It is not proposed that the humidity is changing the E/N ratio directly but, rather, another effect is occurring. This will be discussed later in Section 5.5.1.

An important difference observed in varying the humidity compared to pressure is that as the latter was increased the formation of the different ion species relative to one another did not extensively change. Since water plays a key role in the ionisation pathways of the ions it is proposed that the increase in humidity has led to a change in the equilibrium positions of those reactions. Additionally, the separation of ion species first appears to reduce with an increase in humidity but then later increase when the humidity is increased further. This suggests the presence of more than one process, something that will be investigated in more detail in Section 5.5.2.

5.5   Constant E/N with DMMP

Having completed the full DF sweeps, the assessment was then focussed on to the specific CV sweeps corresponding to the reference E/N environments selected earlier (Section 5.2.3). The properties of intensity, CV position and FWHM of each ion response were collected for analysis.

To provide an overview of the data collected, a compound variable describing the pressure, humidity and magnitude of carrier flow was created and used to plot against the ion intensity of the product ions. The compound variable was used so that separation of all the

responses was possible in a single plot, thereby enabling the isolation of limiting conditions.

The creation of the compound variable is entirely arbitrary but has a near equal sensitivity to the three separate variables. The compound variable, which is referred henceforth as PFH, is calculated as the product of the pressure, flow rate (both normalised to the conditions of the humidity that was recorded) and the natural log of the absolute humidity.

$$PFH = \left(\frac{P}{P_0}\right)\left(\frac{FR}{FR_0}\right)\ell n(abs(H)) \qquad 5.2$$

Where P is the absolute pressure (bar), P_0 is the absolute pressure when the humidity was recorded (bar), FR is the flow rate (l/min), FR_0 is the flow rate when the humidity was recorded (l/min) and H is the humidity in dew point (°C)[1]. Please note that Equation 5.2 can only be used if the dew points of the different readings are either entirely positive or negative.

Figure 5.10 displays the data obtained along with two scenarios that have been highlighted as they lie at the limits of the observed data. No error bars are included since the standard deviation is typically less than the symbol size.

---

[1] Units are explicitly given for the compound variable within the main text (as opposed to the Glossary, Preface IV) because of the use of non-SI units.
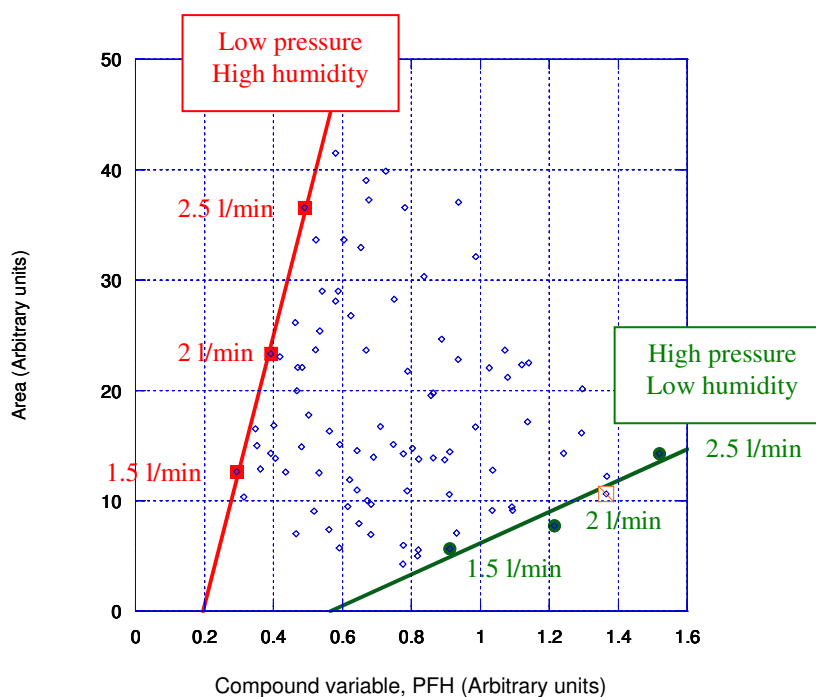
Figure 5.10 Total product ion area at an *E/N* of 110.2 Td at various values of pressure, humidity and carrier flow rate (blue diamonds). Data taken at a pressure of 130 kPa and humidity ~ 2420 ppm (red squares) and data taken at a pressure of 200 kPa and humidity ~ 170 ppm (green circles) is also highlighted. Outlier is labled with orange striked square. Linear lines of best fit are fitted through least squares.

The broad result is that there is a positive correlation of ion intensity with increasing PFH.

The two highlighted scenarios; lowest pressure with highest humidity and highest pressure with lowest humidity, flank the full data set except for a single outlier. These two scenarios represent the limits of the data with a low pressure and high humidity resulting in the greatest product ion intensity for any increase in magnitude of flow. Since the data is from a constant *E/N* environment (110.2 Td) the energy imparted to the ions is equal in all cases The reasons why these two scenarios form the limits of the data will be considered in the following sections but for now Figure 5.10 provides an indication that there are dependencies within the data with the variables investigated at a constant *E/N* environment (results from the two other *E/N* reference conditions are similar to those above).

Approaching the data in this manner has provided an overview but to better explore the information careful isolation of particular parameters is now undertaken. The dependencies relating to the ion intensity, CV position and FWHM of the responses obtained are considered in Sections 5.5.1 - 5.5.3.

5.5.1 Ion intensity at a constant *E/N*

Following on from the general responses presented thus far, ion intensities of the monomer and dimer species are plotted against the humidity of the carrier flow. Investigations holding either the pressure or magnitude of flow constant are given in separate plots. The data presented is at the greatest constant *E/N* reference of 100.2 Td (*i.e.* fully resolved ion species).

Figure 5.11 displays the monomer and dimer ion species at a constant pressure of carrier flow but various magnitudes of flow rate. The data is plotted against humidity of carrier flow.

a)   DMMP, monomer   b)   DMMP, dimer
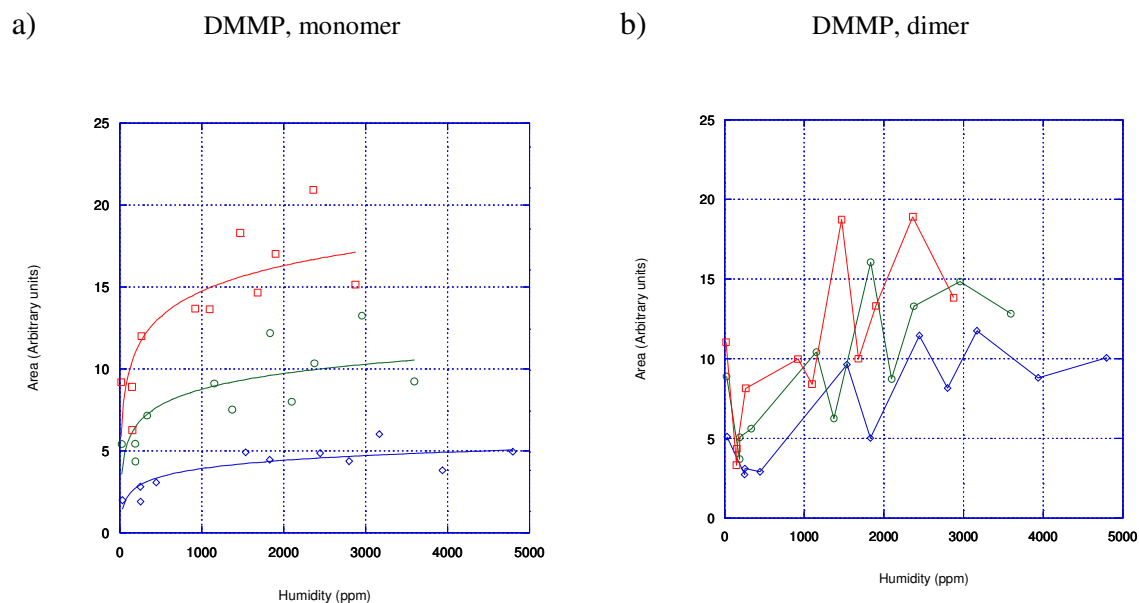
Figure 5.11 Area of ion intensity of the a) monomer and b) dimer DMMP ion species at a carrier flow pressure of 180 kPa and three separate magnitudes with respect to the humidity of the carrier flow; 1.5 l/min (blue diamonds), 2 l/min (green circles) and 2.5 l/min (red squares).

Lines of best fit (logarithmic) have been added to Figure 5.11 a) to help illustrate the trends. Similar lines of best fit were not added to Figure 5.11 b) because the responses at different flow rates did not clearly separate, although it appears that similar trends are in evidence. Also, no errors are included on the plots because the standard deviations of the triplicate readings are smaller than the data icons used.

In both the monomer and dimer responses, an increase in the humidity of carrier flow has led to an increase in the magnitude of ion response. This dependence is, however, not linear and there is a greater sensitivity to a change in humidity at lower concentrations. As the humidity rises, the intensity of ion response levels off. With the monomer this levelling off appears to occur sooner if a lower flow rate has been employed. A similar effect with the dimer response is suggested, but is not as easily observed. The dependence with respect to flow rate suggests that the phenomenon is reliant upon the residence time of the ions within the separation region of the FAIMS sensor. It is proposed that this behaviour of the intensity of ion response with respect to the concentration of water in the carrier flow is a

consequence of the availability of water for the cascade of reactions required to produce the product ions. These reactions have been discussed in detail within Section 2.1. The levelling off represents subsequent interaction with a water molecule becoming redundant since saturation of another quantity (*e.g.* analyte) has occurred. This is supported by the data as investigations with a lower flow rate, and thus higher residence time in the ionisation region, reach this saturation at a lower humidity.

The general increase in ion response between the different flow rates is attributed to the differences in residence time of ions within the separation region. The higher the flow rate the less time ions have had to diffuse to a sensor wall and neutralise (Section 2.9), therefore a greater ion response is observed at higher flow rates. There is increased separation of ion intensities between the monomer species at different flow rates compared to those of the dimer; this is attributed to their respective mobility. The monomer has a greater mobility than the dimer, because it is a lighter and smaller species, and so it has a greater diffusion coefficient and is more sensitive to diffusional losses. This has resulted in the greater partition between the different flow rates, potentially a contributing reason to the levelling of the response.

The greater variation in ion intensity of the monomer ion species at successively greater flow rates is assumed to be a consequence of the decreasing residence time. Less time for diffusional losses, which preferentially removes ions without the exact mobility for detection, to occur means greater variation can be exhibited as a larger range of velocities of ion are present in the population. Dimer ions, with their smaller mobility, exhibit this variation to a smaller extent.

Figure 5.12 displays the monomer and dimer ion species at various pressures but constant magnitude of carrier flow. The errors provided in Figure 5.12 are a single standard deviation of repeated triplicate readings.

a) DMMP, monomer   b) DMMP, dimer
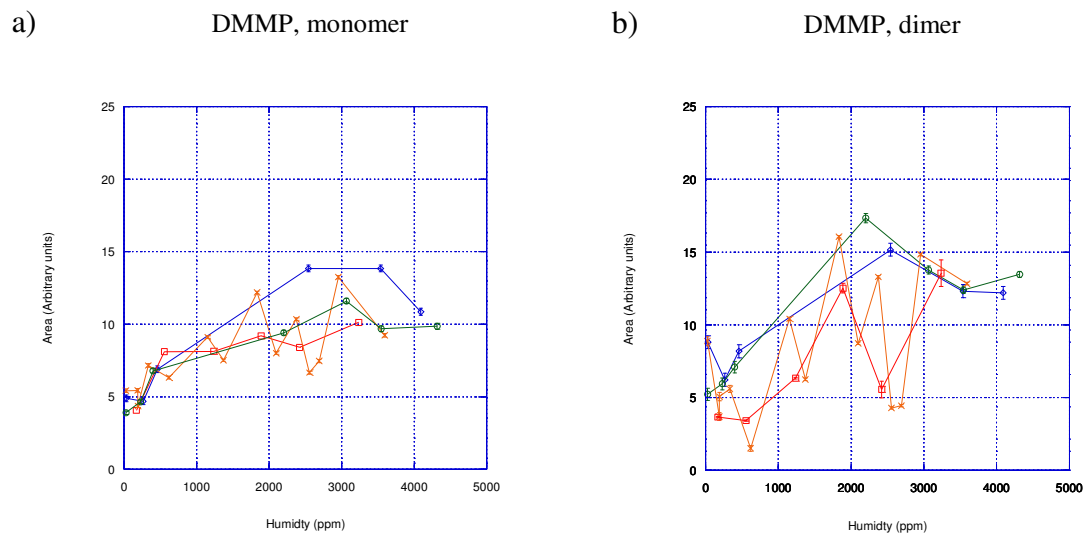
Figure 5.12 Area of ion intensity of the a) monomer and b) dimer DMMP ion species at a carrier flow magnitude of 2 l/min and four separate pressures with respect to the humidity of the carrier flow; 130 kPa (blue diamonds), 150 kPa (green circles), 180 kPa (orange crosses) and 200 kPa (red squares).

Broadly, the same dependence to humidity is observed, for both the monomer and dimer ions species, as in the case where pressure of carrier flow was held constant. The reasons for the behaviour are considered to be the same as presented in the previous case.

With the residence time being equivalent for all the ions within the separation region the ion intensity does not show as great a variation as it did with different flow rates. However, there does appear to be some dependence on carrier flow pressure with lower ion intensities resulting from higher pressures. It was suggested in the preliminary study, with the reactant ions (Section 5.3.1), that an increase in carrier flow pressure led to a decrease in ion intensity. This was attributed to increased losses resulting from greater interaction with neutrals and reactant ions; it is proposed that the same is occurring with the product ions in Figure 5.12.

In obtaining this data a problem with the experimental set-up was revealed. Introducing too great a pressure of carrier gas meant that as the carrier, analyte and humidity flows were combined, a drop in analyte flow across the permeation source was observed. At first this was deemed tolerable, as long as the same quantity of analyte was liberated into the reduced stream the eventual dilution would remain identical. However, a change in pressure above the permeation source would result in a change in permeation rate. It would normally take a number of days for such a change in permeation rate to become stable and it is possible that the change in analyte flow could cause a fluctuation in the ion intensity. Such a variation in analyte flow was observed at carrier flow pressures equal to and greater than 180 kPa. Part way through the study the pressure regulation across the permeation source was amended to prevent this change in analyte flow. The data presented in Figure 5.11 was unaffected by a drop in analyte flow because that data was collected entirely at a carrier flow pressure of 150 kPa. However, the dip in ion intensity between a humidity of 2000 - 3000 ppm for carrier flow pressures of 180 and 200 kPa in Figure 5.12 is attributed to this issue.

5.5.2   Compensation voltage at a constant E/N

Following the previous discussion concerning ion intensity, the focus is now shifted to the CV positions of the observed ion responses and how they are affected by the pressure, humidity and magnitude of carrier flow. All the data presented in this section was obtained at a consistent E/N environment (100.2 Td) to ensure that the results could be correctly attributed to a single parameter.

Figure 5.13 shows the CV position of the peak of monomer and dimer ion responses while employing carrier flows at constant pressure but different flow rates. The data is plotted against the humidity of the carrier flow.

a)   DMMP, monomer   b)   DMMP, dimer
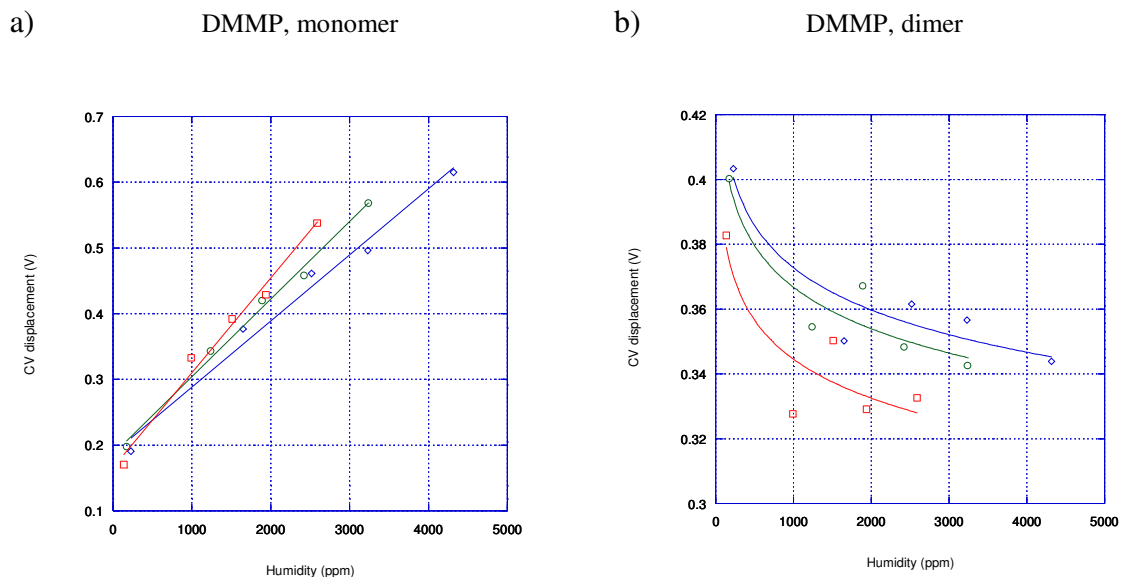
Figure 5.13 CV displacement of the a) monomer and b) dimer DMMP ion species at a carrier flow pressure of 200 kPa and three separate magnitude of carrier flow with respect to the humidity of the carrier flow; 1.5 l/min (blue diamonds), 2 l/min (green circles), and 2.5 l/min (red squares).

Lines of best fit (linear in Figure 5.13 a), logarithmic in Figure 5.13 b)) were added to help describe trends within the different data sets. Also, no error bars are included on the plots because the standard deviations of the triplicate readings are smaller than the data icons used.

As can be seen, the CV displacement of the monomer ion species has a strong linear dependence upon the humidity of the carrier flow. Conversely for the dimer response, the CV displacement decreases with increased flow rate and a greater humidity. To explain this difference it is proposed that the monomer ions are experiencing different levels of solvation with water molecules between the high and low field regions of the applied asymmetric waveform, also known as clustering. Clustering predominantly occurs within

the low field region of the waveform as the field strength in the high field region is typically too great for clustering to be maintained [5, 8, 9, 11].

Krylova *et al*. have previously described clustering with water molecules as the reason for an increasing mobility of DMMP with rising humidity [5]. It has also been stated that DMMP dimers cannot undergo clustering because the only available proton within the ion molecule is required to bind the additional analyte [11]. This would explain why the dimer appears not to experience the same dependence to humidity. Having a different number of water molecules as part of the monomer ion cluster within the low and high field regions of the applied waveform means a different collisional cross section and thus a greater difference in mobility between the regions. A greater mobility difference results in a greater CV displacement (Section 2.7). For clustering to occur the monomer ion will have to experience successful interactions with water molecules, which is more likely in a high humidity environment. Clustering is therefore suggested as an explanation for the proportional and linear dependence on humidity for the monomer.

The dependence on humidity for the dimer appears to describe what was implied in the full DF sweeps of Section 5.4.1; as the humidity increases the CV displacement decreases. This behaviour can be attributed to water being a more polar and larger molecule than either the nitrogen and oxygen molecules present, presented in Table 5.2, and therefore relatively more likely to interact with the ions than the other neutrals present. This would have an effect similar to decreasing the E/N ratio. It is likely something similar has occurred with the monomer ions but it is masked by the larger effect from clustering.

Table 5.2 Permanent dipole moments and bond lengths of H_2O, O_2 and N_2

Molecule	Dipole moment (Debye)	Bond length (pm)
H_2O	1.85 D	197 (O-H)
O_2	-	112 (O=O)
N_2	-	111 (N=N)

While humidity is undoubtedly the dominant factor in influencing the CV displacement, the magnitude of the carrier flow also has a noticeable effect. Like with increasing humidity, the effect of increasing the flow rate is different for the monomer and dimer. This can be explained if the flow rate is considered as affecting the rate at which the ions come into contact with water molecules. The energy imparted to the ions is consistent through the application of a constant E/N environment; the neutrals present, however, will be affected by the magnitude of the carrier flow. A higher flow rate means that the average velocity of neutrals (*e.g.* water) is greater, leading to more interactions with the ions. For the monomer this leads to increased clustering and a greater CV displacement. For the non-clustering dimer it will result in a decreased CV displacement, as observed in Figure 5.13.

Figure 5.14 presents the CV positions of the peak of monomer and dimer ion responses at a constant flow rate but different pressures of carrier flow. The data is plotted against the humidity of the carrier flow.

a)   DMMP, monomer   b)   DMMP, dimer
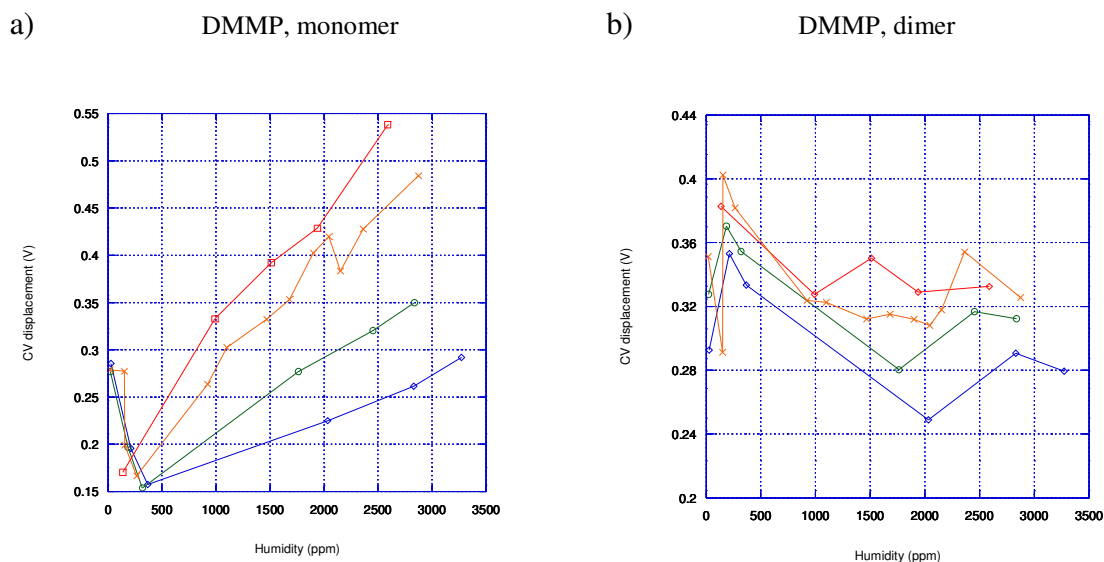
Figure 5.14 CV displacement of the a) monomer and b) dimer DMMP ion species at a carrier flow magnitude of 2.5 l/min and four separate pressures with respect to the humidity of the carrier flow; 130 kPa (blue diamonds), 150 kPa (green circles), 180 kPa (orange crosses) and 200 kPa (red squares).

The responses are similar to those presented within Figure 5.13 with an interesting feature revealed in Figure 5.14 a) concerning the monomer's dependence on humidity, up to 500 ppm. Also, as the carrier flow pressure is increased the CV displacement of both the monomer and dimer ion is greater for a given humidity. No error bars are included in the plots because the standard deviations of the triplicate readings are smaller than the data icons used.

Considering the dimer response first, the reason for the observed dependence on humidity is considered to be the same as with the previously described case for when the pressure of carrier flow was held constant. Furthermore, greater CV displacement with increasing pressure is also explained by considering the velocity of neutrals. Despite the ions experiencing a constant *E/N* environment an increase in pressure will lead to an increase in collisions. For the neutrals, which are not affected by the electric field present, this leads to a decrease in velocity which makes it less likely an ion will interact with a water molecule, thus leading to a greater CV displacement for a given humidity. The increase in CV

200

displacement at low humidity is potentially a result of low levels of humidity affecting the specific identity of the dimer molecular ion cluster, though this has not been confirmed.

Now considering the monomer ion species, at low humidity levels the CV displacement decreases with increased humidity, meets a minimum and then increases for the remainder of the humidity range studied. This behaviour is attributed to the on-set of clustering. An increase in solvation within the low field region of the applied waveform requires a successful interaction between a monomer ion and water molecule within the time that low field conditions are present. Typically the Owlstone FAIMS sensor is running at a high frequency to mitigate against diffusion losses to the sensor walls, so the time available is typically too small for solvation to occur at low humidity. However, with greater humidity it becomes increasingly likely that a monomer ion would encounter a water molecule within the required timeframe. Also, with increased pressure there are a greater number of collisions occurring. It is suggested that the CV displacement of the monomer at first experiences the detrimental effects of the presence of humidity (similar to the dimer) but then, when successful interactions become likely, clustering occurs that results in the observed increase in CV displacement. This is discussed in more detail in Section 5.5.2.1.

The increase in CV displacement, following the on-set of clustering, with greater carrier flow pressure is attributed to greater levels of solvation being possible for a given humidity because the ion is undergoing more collisions, making a successful collision more likely. The detrimental effect of lower neutral velocity is assumed to be masked by the benefits associated with the increased clustering.

5.5.2.1 On-set of clustering

To describe the sudden on-set of clustering observed with an increase of humidity on a range of organophosphates (including DMMP) Krylova *et al* [5]. calculated the number of successful interactions an ion was likely to experience with water molecules within the time of a single low field portion of the applied asymmetric waveform. Their calculation is discussed in more detail within Appendix A but Equation 5.3 results from their methodology.

$$t_{I-W} = \frac{1}{k_R \cdot [H_2O]}$$ 5.3

Where t_{I-W} is the time between a successful interaction between an ion and water molecule in seconds, [H_2O] is the water concentration in molecules/cm^3 and k_R is the collision rate constant (stated as $\sim 1 \times 10^{-9}$ cm^3/molecules·s by Eiceman and Karpas [9]).

The low field region in the Owlstone device exists for approximately 0.027 μs per cycle. Using Equation 5.3 the average number of successful solvations within a low field region, at the pressure and humidity of carrier flow for the four CV displacement minima given in Figure 5.14 a), were calculated (Table 5.3).

Table 5.3 Approximate number of interactions between ion and water molecule during low field conditions of waveform at minimum CV displacement

Carrier flow pressure (kPa)	Average number of successful solvations per low field experienced by each DMMP monomer ion
200	0.23
180	0.40
150	0.34
130	0.40

The number of interactions calculated above is dependent upon the sampling of the carrier flow humidity and is an average across the ion species. Owing to random interactions, within an order of magnitude, it is plausible that some ions will begin to successfully cluster in the low field region of the applied waveform. Following the minimum of the CV displacement the effect attributed to clustering continually increases, in line with the greater expected number of successful interactions through Equation 5.3.

Before the minimum in CV displacement in Figure 5.14 a) it appears the response is less dependent on the pressure of carrier flow but following the minimum there is definite pressure dependence. This implies two separate conditions, before and after the minimum point. Prior to the on-set of clustering, the CV displacement is affected by the increased abundance of the water molecules, similar to the effect witnessed with the non-clustering dimer (Section 5.5.2). After the minimum of CV displacement, the humidity has reached a point where clustering begins to occur. The CV displacement in this clustering region is then directly dependent upon the pressure of the carrier flow since a higher pressure leads to a greater number of interactions.

There is no apparent plateau of CV displacement with increased humidity across the range investigated, which suggests that the potential for greater resolution has not been exhausted. Also, with increased clustering it is expected that the molecular ion will obtain a larger average collisional cross section. This is likely to lead to broadening of the monomer's FWHM and will be discussed in the conclusion to this chapter (Section 5.6).

5.5.3   FWHM at a constant *E*/*N*

As discussed in Section 2.9.1 and investigated in Section 5.3.3, the FWHM is known to be dependent upon the residence time and the number of interactions between constituents within the separation region of the FAIMS device. Figure 5.15 displays the monomer and dimer ion species of DMMP across a range of humidity values and different carrier flow rates.

a)　　　　　　　DMMP, monomer　　　b)　　　　　DMMP, dimer
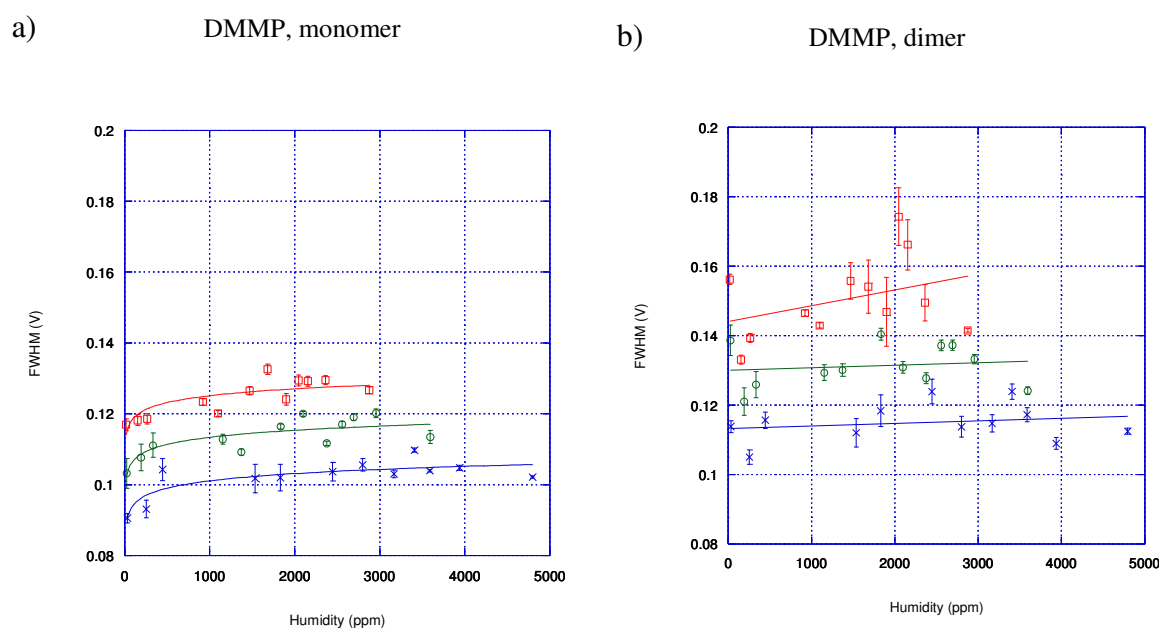
Figure 5.15 FWHM of the a) monomer and b) dimer DMMP ion species at a carrier flow pressure of 180 kPa and three separate magnitudes with respect to the humidity of the carrier flow; 1.5 l/min (blue crosses), 2 l/min (green circles) and 2.5 l/min (red squares).

Lines of best fit (logarithmic in Figure 5.15 a), linear in Figure 5.15 b)) were added to help describe trends within the different data sets. The errors included are a single standard deviation of triplicates.

Considering the monomer, an increase in humidity raises the FWHM observed. There is also a stronger sensitivity to humidity at lower concentrations compared to higher ones. It is suggested that this behaviour mirrors that of the ion intensity of the monomer ion species as described in Section 5.5.1. With an increase in ion intensity there is a greater population

of ions that undergo random interactions; these lead to a broadening of the ion response and, therefore, a larger FWHM.

The monomer's FWHM is dependent on the magnitude of the carrier flow. At greater flow rates, for any particular humidity level, there is an increase in FWHM (as it was described in Section 5.3.3). This is attributed to a reduction of the residence times of ions within the separation region. A lower residence time results in an ion experiencing shorter periods of the filtering waveform, and this leads to a larger proportion of ions with non-ideal mobility characteristics being able to pass on to detection, which increases the FWHM observed.

Considering the FWHM of the dimer ions, there is the same dependence on the flow rate as observed with the monomer ion species. Also, the dependence with humidity appears to be similar to that of the ion intensity of the dimer ions across the same humidity range (Section 5.5.1). The reasons for the observed dimer FWHM, with respect to carrier flow rate and humidity, are considered the same as they were for the monomer ion species. Data that appeared to contradict this claim was obtained at a flow rate of 2.5 l/min and humidity range of ~ 1500 to 2500 ppm. As can be seen in Figure 5.15 b) these data points had a larger error associated with them than points collected under similar conditions. The increased error is attributed to experimental error and so it is unclear how reliable these data points are in understanding the dimer FWHM. As a precaution they were discounted when interpreting the data.

Figure 5.16 displays the monomer and dimer ion species of DMMP across a range of humidity values and several pressures of carrier flow.

a)   DMMP, monomer   b)   DMMP, dimer
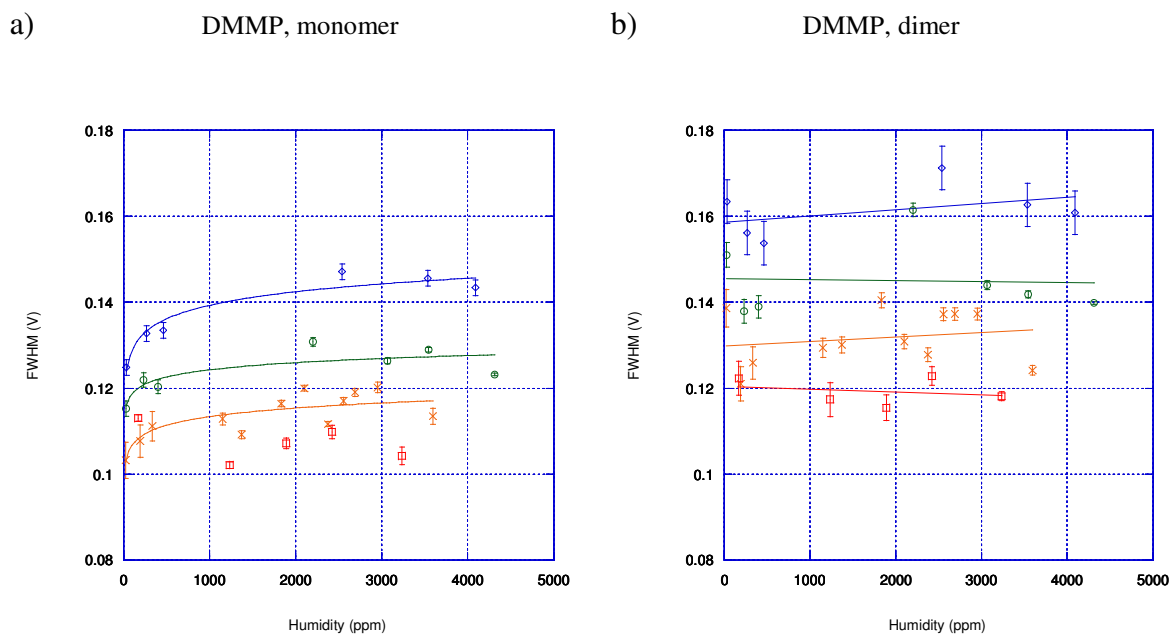
Figure 5.16 FWHM of the a) monomer and b) dimer DMMP ion species at a carrier flow magnitude of 2 l/min and four separate pressures with respect to the humidity of the carrier flow; 130 kPa (blue diamonds), 150 kPa (green circles), 180 kPa (orange crosses) and 200 kPa (red squares).

Lines of best fit (logarithmic in Figure 5.16 a), linear in Figure 5.15 b)) were added to help describe trends within the different data sets. The errors included are a single standard deviation of triplicate readings.

Figure 5.16 a) shows that the monomer FWHM decreases with an increasing pressure of carrier flow. As in the preliminary study (Section 5.3.3), this is attributed to a higher pressure resulting in a greater number of interactions between the ions and neutrals. This, in turn, preferentially removes ions where their mobility deviates from the average of the ion swarm, leading to a smaller FWHM. It is suggested that this same scenario plays out with the dimer ion species (Figure 5.16 b)).

Regarding the humidity dependence of the FWHM of the monomer, it appears that similar arguments to those made when rationalising the response when the pressure was held constant can be applied. However, the FWHM of the dimer generally appears to be less

sensitive to humidity than previously witnessed and the trends between different carrier flow pressures contradict one another. This may be a result of little or no dependence on humidity, additional research would help understand the behaviour.

5.6   Conclusion

This study investigated the effect on the performance of the Lonestar following the variation of the carrier gas parameters: pressure, humidity and flow rate. Of the three parameters it was the dependence of ion response on humidity that was of primary interest. This was mainly because the phenomenon of clustering had been previously reported in the literature but had not yet been observed with an Owlstone FAIMS sensor through a systematic study. An aim was to observe and quantify the on-set of clustering and from the results depicted in Section 5.5.2 it appears that this was accomplished.

Owing to limitations in the experimental set-up the generation of different humidity levels within this study was difficult to specify to a high accuracy. It would be a priority to address this issue if any further investigation was to occur, enabling more targeted research into the humidity ranges of interest.

From the preliminary study it was possible to observe the dependencies between the parameters of the carrier flow and properties of the reactant ion response. A positive correlation was observed for the ion intensity and FWHM with regard to the flow rate of the carrier flow but a negative correlation was observed with the FWHM and carrier flow pressure. A slight negative correlation was also seen between the carrier flow pressure and the ion intensity. No dependence was observed with the modification of either the flow rate or pressure of the carrier flow to the CV position of the reactant ion responses.

The introduction of analyte and humidity to the carrier flow allowed for further relationships to be investigated. Considering the generated DMMP monomer ions, a positive correlation was observed for the CV displacement with the flow rate, pressure and humidity of the carrier flow; however, with the parameters of pressure and humidity this was only above an approximate humidity concentration of 400 ppm. Below this limit the correlation for the pressure and humidity of the carrier flow and CV position was negative. The ion intensity for the DMMP monomer ions was not greatly affected by the modification of any of the three parameters but a slight positive correlation was suggested with the flow rate and humidity of the carrier flow.

The DMMP dimer ions had a different relationship with the parameters of the carrier flow compared to the monomer ions. One difference was that there were no regions of humidity where dependence on a parameter abruptly changed. With regard to the humidity of the carrier flow the ion intensity of the dimer ions had a negative correlation while the CV of the ion response had a slightly positive relationship. The flow rate of the carrier flow had a slight positive correlation between the ion intensity and a negative one with CV. Finally, the pressure of the carrier flow resulted in a positive correlation with the ion intensity of the DMMP dimer ion response but had no effect upon the CV position of the ions, similar to the case with the reactant ions.

An unexpected observation was the relationship between the ion intensity and humidity of the DMMP monomer ions. It was assumed that if there was any effect it would be minor but under some conditions the signal more than doubled in intensity. Further study into the ionisation region, initially independent of a separation region, appears to be warranted. Also, extending the study to investigate more pressures and magnitudes of carrier flows could reveal some hidden structure as yet not observed. This may include limits such as

when the rate of CV displacement, with respect to humidity, no longer increases with greater pressure. This in turn could be used to help better understand the mechanism underlying the relationship.

There are also outstanding issues with understanding the FWHM of the analyte ions. From work by Rorrer and Yost [8] it was expected that the presence of clustering, which is strongly implied by the monomer CV displacement, would be accompanied by an increase in FWHM of the detected ion response. In Figure 5.15, when the carrier flow pressure was held constant, the FWHM of the monomer did show a rise across the humidity range suitable for clustering but the rate of increase was equivalent to that of the dimer, which cannot undergo clustering. There is the possibility that the increase in FWHM resulting exclusively from clustering was masked by the general effect from the presence of water molecules. Furthermore, Figure 5.16 which displays the FWHM at various pressures of carrier flow, again displays a rise in FWHM with humidity for the monomer but then only occasionally with the dimer. The greater variation of the dimer ion response in this plot makes it difficult to make definite judgements and follow-up work is recommended.

With regard to the wider implications of this work, this study used an Owlstone Lonestar unit that had been modified so that the entire flow entered the sample inlet. The normal configuration of a Lonestar is that a sample flow of up to a few hundred ml/min is integrated into a carrier flow for a total flow within the system of around 2 l/min (Section 3.4.1). The carrier flow is typically at a low humidity (*e.g.* ~ 10 ppm) while the sample volume could have a humidity a great deal higher (*e.g.* > 10000 ppm). Taking these example humidity levels of the carrier and sample flows, a total flow of 2 l/min and the sample flows for the six different sample wheel settings of the Lonestar, the resultant

209

values of humidity can be calculated[2]. In Figure 5.17 these values are presented with regard to plots obtained within this chapter relating to the monomer of DMMP's ion intensity and CV position.

a) DMMP, monomer (carrier flow pressure of 180 kPa)   b) DMMP, monomer (flow rate of 2.5 l/min)
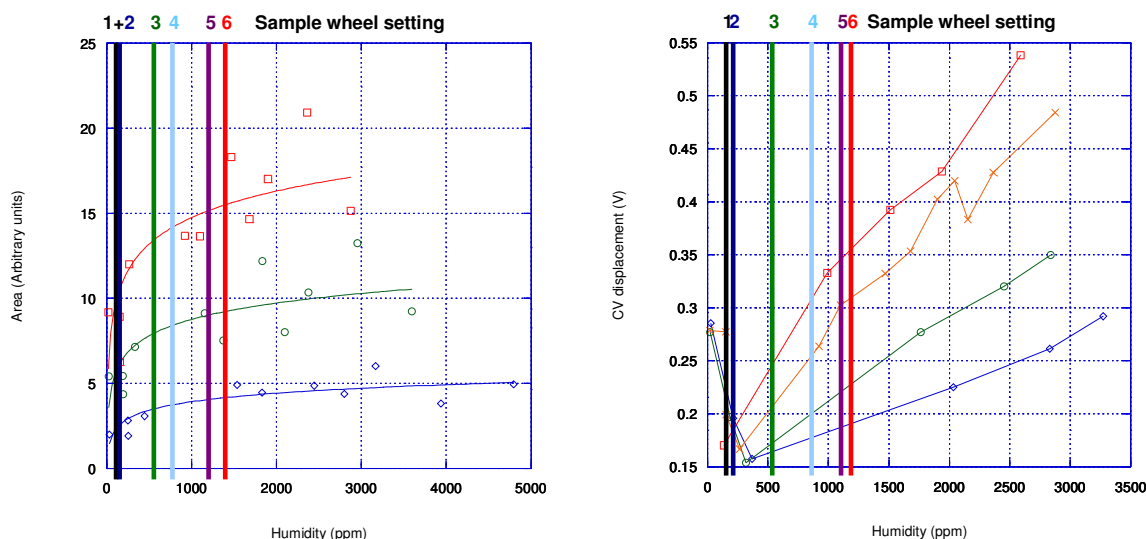
Figure 5.17 Plots originally from a) Figure 5.11 and b) Figure 5.14 with vertical solid lines describing humidity levels of hypothetical scenarios at various Lonestar sample wheel settings.

As can be seen, the selection of the correct sample wheel setting becomes important as the regions of greatest variation occur across the humidity range. The work undertaken now enables the targeting of specific behaviour of DMMP which can be used to permit detection in difficult scenarios. Since DMMP is a recognised simulant for sarin, the most obvious application would be related to homeland defence.

The response of DMMP, as investigated within this study, suggests a number of trends with respect to the investigated parameters of humidity, pressure and magnitude of carrier

---

[2] $[H_2O]_{carrier} = [H_2O]_{sample}\left(\dfrac{flow_{sample}}{flow_{total}}\right) + [H_2O]_{make-up}\left(\dfrac{flow_{make-up}}{flow_{total}}\right)$

where $[H_2O]$ is the humidity concentration.

flow. It is expected that, while the specifics of the dependencies observed will have resulted from the unique character of DMMP, much of the broad behaviour will be common to other analytes. The findings from this study should consequently be possible to exploit in future work with other target compounds.

5.7   References

1.   Nazarov, E.G., Miller, R.A., Eiceman, G.A., and Stone, J.A., *Miniature Differential Mobility Spectrometry Using Atmospheric Pressure Photoionization.* Analytical Chemistry, 2006. **78**(13): p. 4553-4563.
2.   Nazarov, E.G., Coy, S.L., Krylov, E.V., Miller, R.A., and Eiceman, G.A., *Pressure effects in differential mobility spectrometry.* Analytical Chemistry, 2006. **78**(22): p. 7697-7706.
3.   An, X., Eiceman, G., and Stone, J., *A determination of the effective temperatures for the dissociation of the proton bound dimer of dimethyl methylphosphonate in a planar differential mobility spectrometer.* International Journal for Ion Mobility Spectrometry, 2010.
4.   Ewing, R.G., Eiceman, G.A., Harden, C.S., and Stone, J.A., *The kinetics of the decompositions of the proton bound dimers of 1,4-dimethylpyridine and dimethyl methylphosphonate from atmospheric pressure ion mobility spectra.* International Journal of Mass Spectrometry, 2006. **255-256**: p. 76-85.
5.   Krylova, N., Krylov, E., Eiceman, G.A., and Stone, J.A., *Effect of moisture on the field dependence of mobility for gas-phase ions of organophosphorus compounds at atmospheric pressure with field asymmetric ion mobility spectrometry.* Journal of Physical Chemistry A, 2003. **107**(19): p. 3648-3654.
6.   Miller, R.A., Nazarov, E.G., Eiceman, G.A., and King, A.T., *A MEMS radio-frequency ion mobility spectrometer for chemical vapor detection.* Sensors and Actuators a-Physical, 2001. **91**(3): p. 301-312.
7.   Krylov, E.V. and Nazarov, E.G., *Electric field dependence of the ion mobility.* International Journal of Mass Spectrometry, 2009. **285**: p. 149 -156.
8.   Rorrer III, L.C. and Yost, R.A., *Solvent vapor effects on planar high-field asymmetric waveform ion mobility spectrometry.* International Journal of Mass Spectrometry, 2010.
9.   Eiceman, G.A. and Karpas, Z., *Ion Mobility Spectrometry.* Second ed. 2005: Taylor & Francis. 350.
10.   Good, A., Durden, D.A., and Kebarlf, P., *Ion-Molecule Reactions in Pure Nitrogen and Nitrogen Containing Traces of Water at Total Pressures 0.5 - 4 torr. kinetics of Clustering Reactions Forming H+(H2O)n.* The Journal of Chemical Physics, 1969. **52**(1): p. 212 - 221.
11.   Shvartsburg, A.A., *Differential Ion Mobility Spectrometry.* 2009, Boca Raton: CRC Press, Taylor and Francis Group.